Test of the Independence Hypothesis by Angular Distribution Measurements*

D. M. Montgomery† and N. T. Porile
Department of Chemistry, Purdue University, Lafayette, Indiana 47907
(Received 24 October 1970; revised manuscript received 4 March 1970)

Angular distributions, average projected ranges, and cross sections for the production of ^{137m}Ce and ^{137g}Ce from the ^{136}Ba(^{4}He, $3n$) and ^{137}Ba(^{3}He, $3n$) reactions have been measured over the energy intervals 27–44 and 14–33 MeV, respectively. The average ranges were found to be consistent with a compound-nuclear process over the entire energy interval for both reactions. The isomer ratios are in good agreement with a calculation based on the spin-dependent statistical theory. Comparison is made with previous cross-section and isomer-ratio measurements, and various discrepancies are discussed. The angular distributions were analyzed to give the average total kinetic energy of the neutrons and photons emitted in the reactions. Comparison of these quantities at the same excitation energy and angular momentum of the compound nuclei shows that they are equal within the limits of error and thereby confirms the independence hypothesis. The observed differences in the average photon energies for reactions leading to ^{137m}Ce and ^{137g}Ce are quantitatively related to the difference in the average angular momentum of compound nuclei leading to each isomer.

I. INTRODUCTION

One of the underlying assumptions of compound-nuclear reactions is that the decay of the compound nucleus is independent of its mode of formation. The excited nucleus has a sufficiently long lifetime that all correlations between the entrance and exit channels are lost except for those associated with the conservation of energy, angular momentum, and other invariants. The independence hypothesis was first tested by Ghoshal[1] by means of excitation function measurements for reactions involving the formation of a particular compound nucleus in two different ways. This type of experiment is not particularly sensitive to the details of the deexcitation process since the yield of the observed product is an integral over many such processes. Moreover, recent experiments of this kind[2,3] indicate that angular momentum effects can complicate the interpretation of the results. A more sensitive test of the independence hypothesis involves a comparison of the energy spectra of particles emitted by a given compound nucleus formed in different ways. A recent study[4] confirmed the independence hypothesis on the basis of the energy spectra of protons and α particles emitted from the compound nucleus ^{75}Br, formed with ^{12}C and ^{16}O ions.

In the present work the independence hypothesis is tested by means of a different experiment than those that have been used heretofore: the angular distribution of the recoil product of a compound-nuclear reaction. Such a measurement permits a determination of the average total kinetic energy of the emitted nucleons and photons.[5,6] A sensitive test of the independence hypothesis can be performed if this energy partition is determined for a particular deexcitation mode of a compound nucleus formed in two different ways.

The reactions selected for this work were ^{136}Ba(^{4}He, $3n$) and ^{137}Ba(^{3}He, $3n$). The product consists of an isomeric pair, ^{137m}Ce($t_{1/2} = 34.4\ h, I\pi = \frac{11}{2}+$) and ^{137g}Ce($t_{1/2} = 9.0\ h, I\pi = \frac{3}{2}+$). The use of ^{4}He and ^{3}He projectiles minimizes the difference in the angular momenta of the respective compound nuclei. The study of a reaction involving isomeric products simplifies the evaluation of angular momentum effects and is also of intrinsic interest to a more complete understanding of such effects in compound-nuclear reactions.

In order to test the independence hypothesis it must first be established that the reactions in question proceed via compound-nucleus formation. We have measured the average projected ranges of the reaction products in order to determine the energy interval where the compound-nuclear process predominates. In the course of performing these measurements, the excitation functions and isomer ratios were also determined and the latter were compared with the spin-dependent statistical theory. The excitation functions and isomer ratios for the ^{136}Ba(^{4}He, $3n$) reaction have previously been measured by Kiefer and Street[7] (KS) and by Matsuo, Matuszek, Dudey, and Sugihara (MMDS).[8] There were a number of discrepancies between their results. The isomer ratios reported by KS were about 30% lower than those of MMDS. In addition, a shift of approximately 3 MeV in the bombarding energy scale is necessary to obtain agreement between their cross sections. The report of MMDS also includes a measurement of the average recoil ranges and that of KS includes the isomer ratios and cross sections for the ^{137}Ba(^{3}He, $3n$) reaction.

II. EXPERIMENTAL

A. Ranges and Cross Sections

The average range measurements were performed in the same manner as reported in previous communications from this laboratory.[9,10] The target assembly consisted of the conventional stacked-foil arrangement with 6–8 targets and corresponding catchers. The target stack also included additional aluminum foils of various thicknesses to degrade the ^{3}He or ^{4}He beam. The energy of the beam at various positions along the target assembly was calculated from the incident beam energy and an appropriate range-energy relationship.[11] The target stack was mounted in an evacuated water-cooled target holder which also served as a Faraday cup for measurement of beam current.

The irradiations were performed with the ^{3}He and ^{4}He beams of the 60-in. cyclotron at Argonne National Laboratory for periods of 1 to 2 h. The beam intensity was limited to less than 0.3 μA because the $Ba(NO_3)_2$ targets tended to melt and fuse at higher beam currents.

Enriched ^{136}Ba(92.9%) and ^{137}Ba(89.6%) were obtained from Oak Ridge National Laboratory. The targets were prepared from this material by electrophoresis of a fine suspension of $Ba(NO_3)_2$ in acetone onto 0.8 mil-thick aluminum foil of high purity (99.999%) using a modification of a procedure described by Bjørnholm.[12] Target thicknesses were determined by weighing a known area and averaged about 1 mg/cm^2. The catcher foils also consisted of the same pure aluminum.

After irradiation the Ce activities were separated using a modification of a previously described chemical procedure.[13] The targets and catchers were dissolved in a mixture of HCl and HNO_3 containing Ce^{+3} and La^{+3} carriers. The Ce^{+3} was oxidized to Ce^{+4} and precipitated with 6 M NaOH. The $Ce(OH)_4$ was washed, dissolved in a mixture of HNO_3 and $NaBrO_3$, extracted into methyl isobutyl ketone, and then back-extracted into H_2O containing a few drops of H_2O_2. The Ce^{+3} was precipitated as $Ce_2(C_2O_4)_3 \cdot 9H_2O$ and weighed to determine the chemical yield.

The decay of the ^{137}Ce activities was determined with several thin NaI(Tl) detectors having beryllium windows. The detectors were used in conjunction with single-channel analyzers set to accept the K x rays from La and Ce. The x-ray detectors were calibrated with ^{137}Ce samples that had been standardized with an x-ray detector of known efficiency. Differences in efficiency due to self-absorption of the x rays were found to be negligible for sample thicknesses (~9 mg/cm^2) used in this work.

The decay scheme[14] of ^{137m,g}Ce is shown in Fig. 1. Cerium K x rays from the metastable product result from the 255-keV transition. Taking the internal conversion coefficient[14] and fluorescence yield[15] into account, there are 0.53 K x rays per disintegration. In the case of ^{137g}Ce, the x rays result from the decay by electron capture to ^{137}La. Neglecting the x rays from the internal conversion of the 446-keV γ ray (~0.04%) and using a value[15] of 0.89 for the fraction of electron capture transitions occurring as K capture, the number of K x rays per disintegration is 0.80.

The decay curves were analyzed by a least-squares program appropriate to the particular parent-daughter system of interest, described in a recent publication from this laboratory.[16] This program also calculated the cross sections and average projected ranges from the disintegration rates and included a correction for decay of ^{137m}Ce during irradiation.

B. Angular Distributions

The experimental procedure and apparatus for angular distribution studies have been described previously.[17,18] Thin targets are irradiated in an evacuated chamber. The product nuclei recoil out of the target in a forward cone and are stopped by a circular catcher foil placed a known distance from the target. The catcher foil is cut into concentric rings each of which corresponds to a particular angular interval and the radioactivity of

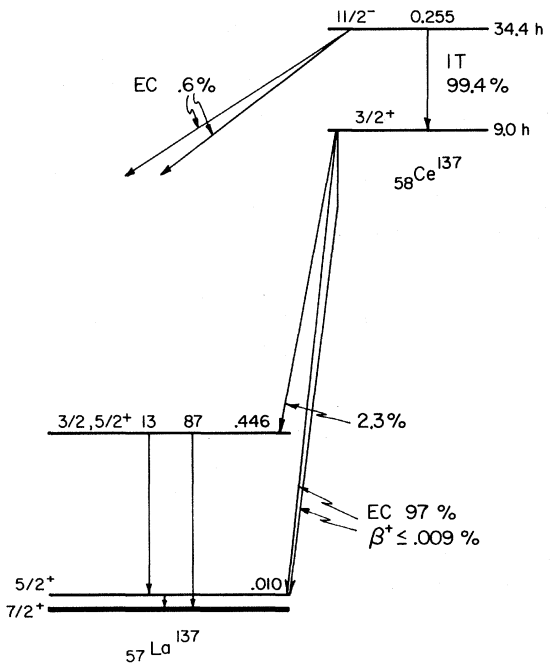

FIG. 1. Decay scheme of ^{137}Ce.

each ring is assayed following chemical separation of cerium.

Thin targets, ranging from 5 to 15 $\mu g/cm^2$, were prepared by molecular plating.[19] Fifty microliters of a solution containing 10 to 20 μg of $Ba(NO_3)_2$ were placed in a cell containing approximately 20 ml isopropyl alcohol. A rotating platinum electrode assembly was used to deposit $Ba(NO_3)_2$ on 0.8 mil-thick pure aluminum. The Al foil served as the cathode and the cell was operated at 250 V for approximately 1 h. Irradiations lasted from 2 to 3 h at beam intensities from 0.1 to 0.3 μA. The beam was collimated before entering the chamber by 0.95- and 0.48-cm apertures. A 0.32-cm collimator located just in front of the water-cooled target holder further defined the beam. Before inserting the target foil, alignment experiments were performed to insure that the beam passed through the center of the target and catcher foils. The beam was degraded to the desired energy by placing Al foils in front of the collimators. The catcher foil consisted of the same high-purity aluminum as the target backing. After irradiation, it was cut into 10 concentric rings and Ce was separated from each foil and assayed in the manner described above.

The effects of target thickness and collimator size on the angular distribution were investigated for the $(^4He, 3n)$ reaction. The target-thickness effect was determined by irradiating targets of 5.5 and 10.0 $\mu g/cm^2$ at 39.2- and 39.0-MeV bombarding energy, respectively, with a 0.32-cm collimator at the target. The collimator effect was studied by irradiating a 12.0-$\mu g/cm^2$ target with a 0.16-cm collimator at 39.1 MeV. The resulting angular distributions of ^{137m}Ce are shown in Fig. 2. The various curves have been normalized to the same area. It is seen that there is no broadening of the angular distribution due to target thickness for the thin targets used in this experiment. The mean angles obtained for target thicknesses of 5.5 and 10.0 $\mu g/cm^2$ were 10.1 and 10.0°, respectively. The ^{137g}Ce angular distributions showed the same insensitivity to target thickness as those of ^{137m}Ce. The mean recoil angle of ^{137m}Ce from the experiment with the 0.16-cm collimator was 10.8°. The widening of the angular distribution for a smaller collimator is opposite to the expected effect and must be due to an experimental uncertainty for this particular bombardment. A subsequent[20] test of the collimation effect using the same apparatus and similar experimental conditions showed that collimation effects on the angular distributions of $^{137m,g}Ce$ are negligible.

III. RESULTS

The average recoil range projected in the direction of the beam is given by

$$R = FW, \tag{1}$$

where F is the fraction of the total activity due to a given nuclide found in the catcher foil and W is the target thickness. The application of Eq. (1) is based on the assumption that the production cross section is constant throughout the target. This assumption is valid in view of the negligible energy degradation of the beam in the thin targets used in this experiment. The experimental results for the average projected ranges, cross sections, and isomer ratios for the $^{136}Ba(^4He, 3n)$ and $^{137}Ba(^3He, 3n)$ reactions are given in Table I.

The standard deviations of the isomer ratios in Table I were obtained from a least-squares fit to the decay data. They only represent the statistical uncertainty in the activity measurements and do not reflect possible systematic errors in the decay scheme. The standard deviations from the least-squares fit were less than 5% in all cases. The cross section and average range measurements are subject to errors in target thickness and gravimetric yields as well as the statistical uncertainties in the activities. Target thicknesses are not expected to vary more than 10% in uniformity. The uncertainties in chemical yields are

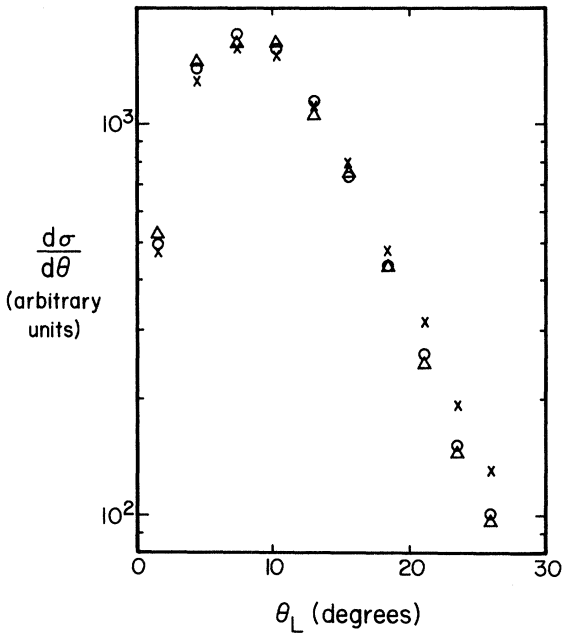

FIG. 2. Dependence of the angular distribution of ^{137m}Ce from the $(^4He, 3n)$ reaction on target thickness and collimator size. 0 – 39.0 MeV, 0.32-cm collimator, and 10.0-$\mu g/cm^2$ target; Δ-39.2 MeV, 0.32-cm collimator and 5.5-$\mu g/cm^2$ target; x-39.0 MeV, 0.16-cm collimator, and 12.0-$\mu g/cm^2$ target. The curves are normalized to the same area.

probably less than 5%. The random errors from all sources for the cross sections and average ranges are estimated to be less than 15%.

Contributions to the ^{137}Ce activities in the ^{3}He bombardments are possible from the ^{138}Ba(^{3}He, $4n$) reaction which has a Q value of −19.5 MeV. The enriched ^{137}Ba contained 9.6% ^{138}Ba as compared with 17.4% in the work of KS.[7] They estimated a maximum contribution of 5 mb due to ^{138}Ba. The contribution due to ^{138}Ba should consequently be only about half this amount in the present work and it has been neglected.

The total cross sections for the ^{136}Ba(^{4}He, $3n$) and ^{137}Ba(^{3}He, $3n$) reactions are plotted and compared with previous measurements in Figs. 3 and 4. The excitation function for the (^{4}He, $3n$) reaction has its maximum at about the same energy as that of KS, but at about 3 MeV above that reported by MMDS. It would appear that the energy calibration of the cyclotrons used by MMDS differs significantly from that of KS and the present work. The shape of the (^{3}He, $3n$) excitation function agrees fairly well with the work of KS.

A striking discrepancy between the present work and the earlier reports is the difference in the magnitude of the cross sections. The (^{4}He, $3n$) excitation function rises to its maximum of about 1300 mb at 39 MeV. This value is about 2.0 and 2.5 times larger than the maximum values reported by MMDS and KS, respectively. The (^{3}He, $3n$) excitation function has a maximum cross section of 560 mb at 25 MeV which is about twice the corresponding peak value from the work of KS. These differences can largely be attributed to the different counting techniques and corresponding radiation abundances used in the various studies. We refer to Fig. 1 for a discussion of the various radiations that have been used to detect ^{137m,g}Ce. The radioactivity measurements of MMDS were based on the L x rays of ^{137m,g}Ce while those of KS involved the 446-keV γ ray from the decay of ^{137g}Ce.

In order to resolve the difference between the present results and those of KS, the disintegration rates of several ^{137m,g}Ce samples were determined from measurements of both the 446-keV γ ray and K x rays. The intensity of the 446-keV photons was assayed with a calibrated 3 × 3-in. NaI(Tl) detector. The disintegration rates of the ^{137}Ce isomers were found to be 30% lower than those obtained from the K x-ray measurements. In order to bring the γ-ray measurements into agreement with K x-ray results it is necessary to assume a

TABLE I. Experimental cross sections, average ranges, and isomer ratios for the ^{136}Ba(^{4}He, $3n$) and ^{137}Ba(^{3}He, $3n$) reactions.

Bombarding energy (MeV)	^{137g}Ce σ (mb)	^{137g}Ce R (μg/cm^2)	^{137m}Ce σ (mb)	^{137m}Ce R (μg/cm^2)	Isomer ratio σ_m/σ_g
		Bombardment A ^{137}Ba(^{3}He, $3n$)			
33.4	76	74	262	83	3.43 ± 0.13
30.2	96	77	310	86	3.24 ± 0.10
26.8	130	76	373	77	2.93 ± 0.09
25.0	158	73	382	74	2.42 ± 0.04
21.7	164	82	266	81	1.63 ± 0.02
18.1	88	66	92	63	1.04 ± 0.01
		Bombardment B ^{137}Ba(^{3}He, $3n$)			
28.6	94	68	354	71	3.75 ± 0.15
23.4	161	58	372	58	2.31 ± 0.04
20.0	136	53	204	52	1.50 ± 0.04
18.2	93	50	107	51	1.15 ± 0.01
16.2	37	47	33	47	0.89 ± 0.01
14.2	4.0	41	2.8	42	0.70 ± 0.01
		Bombardment C ^{136}Ba(^{4}He, $3n$)			
44.2	109	131	947	134	8.71 ± 0.32
41.4	145	137	1048	144	7.25 ± 0.30
39.0	185	121	1059	127	5.71 ± 0.40
36.8	203	110	965	116	4.76 ± 0.37
34.8	168	115	715	118	4.26 ± 0.19
32.8	143	115	492	116	3.43 ± 0.08
29.6	48	94	120	90	2.51 ± 0.08
27.1	42	94	11.3	95	2.66 ± 0.13

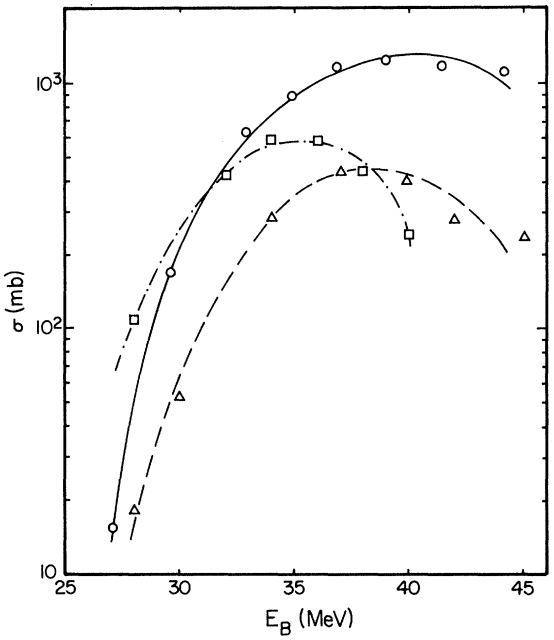

FIG. 3. Excitation function for the ^{136}Ba(^{4}He, $3n$)-^{137m,g}Ce reaction. Circles, squares, and triangles represent cross sections from this work, Refs. 8 and 7, respectively.

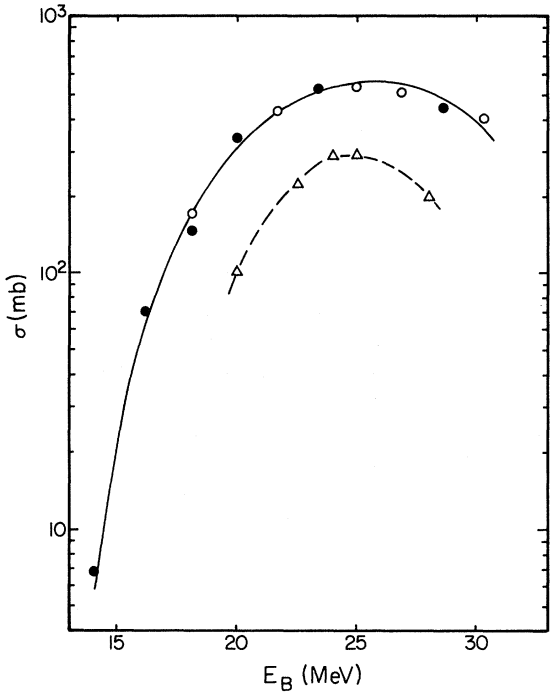

FIG. 4. Excitation function for the ^{137}Ba(^{3}He, $3n$)-^{137m,g}Ce reaction. The circles are from this work and the triangles from Ref. 7.

branching ratio of 1.8% for the population of the 446-keV level in ^{137}La instead of the adopted[14] value of 2.3%. Since KS used an even higher branching ratio of 3% in computing their cross sections, most of the discrepancy can be attributed to this difference.

The discrepancy with the results of MMDS can be attributed to the adopted value of the L-shell fluorescence yield, ω_L. The MMDS cross sections are inversely proportional to ω_L and there are conflicting values in the literature, $\omega_L = 0.092$[21] and $\omega_L = 0.17$.[15] The work of MMDS assumed a value of 0.17 for ω_L. Their (^{4}He, $3n$) peak cross section would be approximately the same as the present value if $\omega_L = 0.092$ were used instead.

Another factor suggesting that the present cross sections are valid is that the (^{4}He, $3n$) peak cross

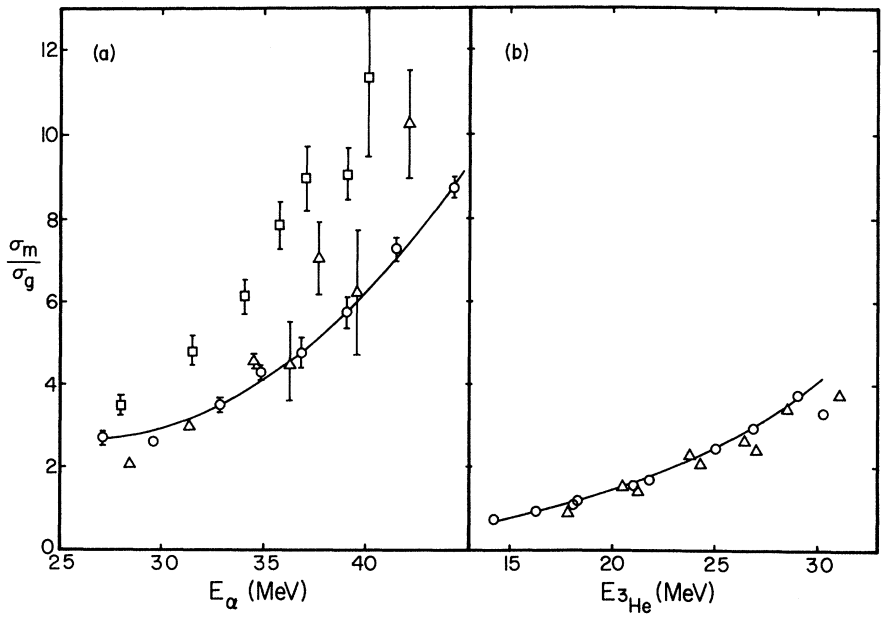

FIG. 5. Isomer ratios for the (^{4}He, $3n$) and (^{3}He, $3n$) reactions are given in (a) and (b), respectively. The circles are from this work, squares from Ref. 8, and triangles from Ref. 7.

sections reported by KS and MMDS correspond to only 0.26 and 0.35 of the total reaction cross section, respectively. By contrast, the present results indicate that at peak energies this reaction accounts for 65% of the total reaction cross section. In arriving at these estimates the total reaction cross section was computed on the basis of the optical model by use of the ABACUS-2 code.[22] Previous measurements of (^{4}He, $3n$) reaction cross sections in the mass region of interest indicate that at peak energies this reaction accounts for 60–70% of the total reaction cross section.[23,24]

A comparison of the various isomer ratio measurements is shown in Fig. 5. In the case of the (^{4}He, $3n$) reaction, the isomer ratios of MMDS are from 30 to 50% higher than our values. The values of KS agree fairly well with the present values below about 40 MeV, but become larger at higher energies. There is good agreement between the isomer ratios for the (^{3}He, $3n$) reaction as reported by KS and the present work over the entire energy range.

The angular distribution data, which are available from the authors on request, were used to obtain for each reaction the values of the mean laboratory recoil angle, $\langle\theta_L\rangle$, and those of $\langle\tan^2\theta_L\rangle$. The equations by which these quantities were calculated from the measured disintegration rates, D_i, are:

$$\langle\theta_L\rangle = \sum_i D_i \Delta\theta_i \langle\theta_i\rangle / \sum D_i \Delta\theta_i \tag{2}$$

and

$$\langle\tan^2\theta_L\rangle = \sum_i D_i \Delta\theta_i \langle\tan^2\theta_i\rangle / \sum_i D_i \Delta\theta_i \ . \tag{3}$$

The summations are over the i rings of the catcher foil, $\Delta\theta_i$ is the angular interval corresponding to the ith ring, and $\langle\theta_i\rangle$ and $\langle\tan^2\theta_i\rangle$ are the mean values of these quantities for the ring in question.

The results are summarized in Table II. The uncertainties in the $\langle\theta_L\rangle$ values are approximately 0.1–0.3° and arise from the statistical uncertainty in the disintegration rates, as well as minor errors in the chemical yield determinations and alignment procedures.

TABLE II. Values of quantities derived from angular distributions.

Isomer	Bombarding energy (MeV)	$E_{c.m.}+Q$ (MeV)	$\langle\theta_L\rangle$ (deg)	$\langle\tan^2\theta_L\rangle$	T_n (MeV)	T_γ (MeV)
			^{136}Ba(^{4}He, $3n$)			
m	43.6	17.4	11.3	0.0574	14.0 ± 0.3	3.4 ± 0.3
g	43.6	17.7	12.4	0.0673	16.2 ± 0.8	1.5 ± 0.8
m	41.3	15.2	10.8	0.0522	12.1 ± 0.2	3.1 ± 0.2
g	41.3	15.5	11.7	0.0603	13.8 ± 0.7	1.7 ± 0.7
m	39.2	13.2	10.0	0.0437	9.7 ± 0.1	3.5 ± 0.1
g	39.2	13.5	10.8	0.0503	11.1 ± 0.6	2.4 ± 0.6
m	39.1	13.1	10.8	0.0534	11.7 ± 0.2	1.4 ± 0.2
g	39.1	13.4	11.0	0.0542	11.9 ± 0.6	1.5 ± 0.6
m	39.0	12.9	10.1	0.0446	9.8 ± 0.2	3.1 ± 0.2
g	39.0	13.2	10.5	0.0466	10.2 ± 0.5	3.0 ± 0.5
m	36.1	10.2	9.8	0.0421	8.6 ± 0.2	1.6 ± 0.2
g	36.1	10.5	10.1	0.0442	9.0 ± 0.5	1.5 ± 0.5
m	33.3	7.5	9.5	0.0390	7.5 ± 0.2	0.0 ± 0.2
g	33.3	7.8	10.1	0.0434	7.8 ± 0.4	0.0 ± 0.3
			^{137}Ba(^{3}He, $3n$)			
m	32.5	20.5	16.0	0.1284	16.4 ± 0.3	4.1 ± 0.3
g	32.5	20.8	16.9	0.1440	18.2 ± 0.7	2.6 ± 0.9
m	28.0	16.1	15.4	0.1187	13.2 ± 0.3	2.9 ± 0.3
g	28.0	16.4	16.2	0.1336	14.7 ± 0.7	1.7 ± 0.7
m	27.8	15.9	15.1	0.1164	12.9 ± 0.3	3.0 ± 0.3
g	27.8	16.2	15.3	0.1174	13.0 ± 0.6	3.2 ± 0.6
m	27.6	15.8	15.5	0.1202	13.2 ± 0.3	2.6 ± 0.3
g	27.6	16.1	16.1	0.1315	14.3 ± 0.7	1.8 ± 0.7
m	24.3	12.5	15.7	0.1213	11.7 ± 0.1	0.8 ± 0.2
g	24.3	12.8	15.9	0.1242	11.9 ± 0.6	0.9 ± 0.6
m	20.3	8.6	15.0	0.1059	8.6 ± 0.2	0.0 ± 0.4
g	20.3	8.9	15.2	0.1082	8.8 ± 0.4	0.1 ± 0.4

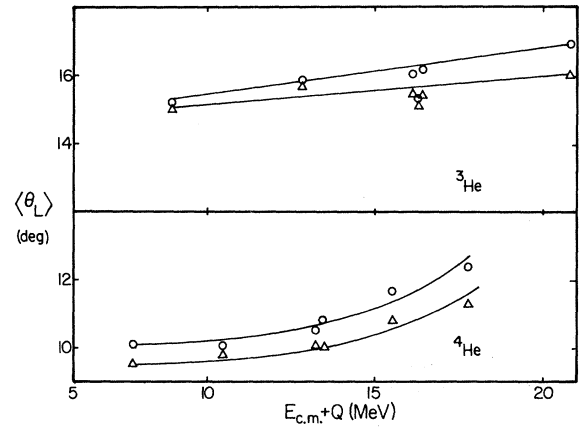

FIG. 6. Average recoil angles of ^{137m,g}Ce from the (^{3}He, 3n) and (^{4}He, 3n) reactions. The circles refer to ^{137g}Ce and triangles to ^{137m}Ce.

The mean angles are plotted as a function of the available energy, $E_{c.m.}+Q$, in Fig. 6. The Q values were determined from the nuclidic masses compiled by Mattauch, Thiele, and Wapstra[25] and $E_{c.m.}$ is the c.m. bombarding energy. The various trends displayed by these data are readily explainable. The gradual increase of $\langle\theta_L\rangle$ with energy arises from the fact that the recoil velocity due to neutron emission increases more rapidly with energy than the velocity of the compound nucleus. For a given value of the available energy the $\langle\theta_L\rangle$ from ^{3}He irradiations are some 3–5° larger than those for ^{4}He. This difference is merely a consequence of the larger forward momentum imparted to the compound nucleus in ^{4}He bombardments. The $\langle\theta_L\rangle$ of ^{137m}Ce are uniformly larger than those of ^{137g}Ce, the difference at a given energy amounting to close to 1°. This difference reflects differences in the partition of the available energy between neutrons and photons and is discussed in more detail below.

IV. DISCUSSION

A. Comparison of Average Ranges with Compound-Nuclear Values

The average projected ranges of the (^{4}He, 3n) and (^{3}He, 3n) reaction products are plotted as a function of projectile energy in Fig. 7 and may be compared with values based on a compound-nuclear mechanism. Reactions of this type involve complete momentum transfer from projectile to compound nucleus. The product nucleus recoils with an average kinetic energy given by the formula

$$E_R = E_B \frac{A_B A_R}{(A_T + A_B)^2}, \tag{4}$$

where E_R is the recoil energy, E_B the bombarding energy, and A_T, A_B, and A_R are the masses of the target, bombarding particle, and recoil nucleus, respectively. Theoretical ranges represented by the dashed lines in Fig. 7 are based on the stopping theory of Lindhard, Scharff, and Schiøtt (LSS)[26] and refer to a $Ba(NO_3)_2$ stopping medium.

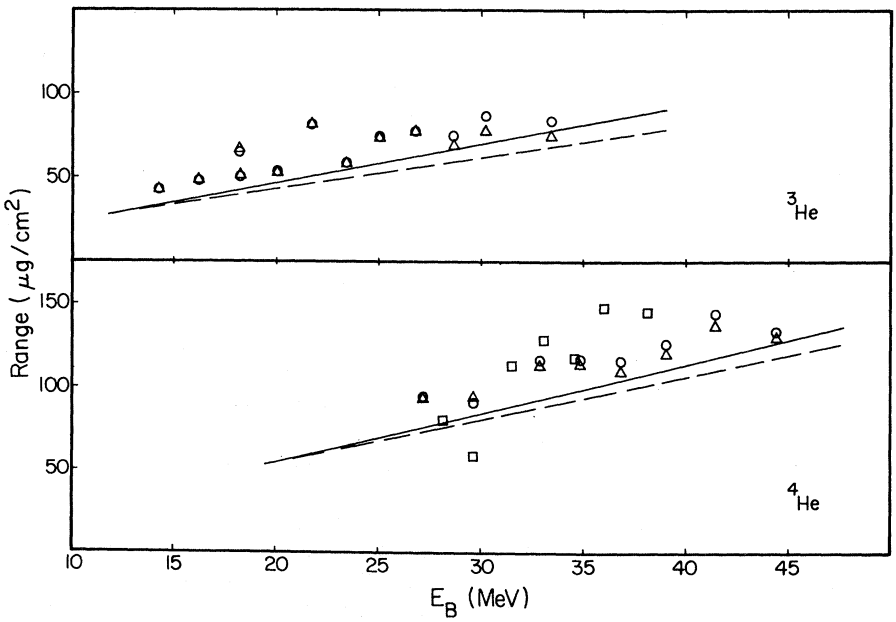

FIG. 7. Average projected ranges of the ^{136}Ba(^{4}He, 3n) and ^{137}Ba(^{3}He, 3n) reaction products. The circles represent ^{137m}Ce and the triangles ^{137g}Ce. The squares are from Ref. 8. The dashed line is the LSS range-energy relation. The solid line is the LSS range corrected for neutron evaporation.

The LSS ranges were corrected for the effect of neutron evaporation as discussed elsewhere[27] and are represented by solid lines in Fig. 7. The corrections increased the ranges by as much as 6 and 12% for the ^{4}He- and ^{3}He-induced reactions, respectively. The average ranges of both the (^{4}He,3n) and (^{3}He, 3n) reaction products increase with bombarding energy in a manner that parallels the energy dependence of the corrected LSS curves although the actual values are some 10% larger than the latter.

If direct interactions made significant contributions to these reactions, the ranges would be substantially lower than the LSS values and would not increase with bombarding energy. It is difficult to make an accurate evaluation of the ranges expected for such a process in the absence of detailed information about the reaction mechanism. However, approximate estimates can be readily presented. For example, if the (^{4}He, 3n) reaction were to involve a stripping process in which two high-energy neutrons are emitted in the forward direction while the third neutron is isotropically evaporated with lower energy, the expected range at 40 MeV would be approximately 50 μg/cm^2. On the other hand, if a knock-on-mechanism in which a single high-energy neutron is emitted in the forward direction and the two remaining neutrons are isotropically evaporated with low kinetic energies is postulated, the expected range is 70 μg/cm^2. Both values are substantially lower than the compound-nuclear value, 110 μg/cm^2. The difference between the estimated direct interaction ranges and the measured values, coupled with the fact that the former do not increase with bombarding energy, indicates that the compound-nuclear mechanism predominates. The same conclusion applies to the ^{3}He-induced reaction.

Also included in Fig. 7 are the average projected ranges reported by MM.[8] Although these data differ by as much as 40% from the present values and scatter pronouncedly, the over-all trend is similar to that reported here.

B. Comparison of the Excitation Functions of ^{3}He- and ^{4}He-Induced Reactions

A comparison of the (^{4}He, 3n) and (^{3}He, 3n) reaction cross sections can be used to determine the relative importance of compound-nucleus formation in ^{3}He- and ^{4}He-induced reactions. Let us assume that the compound-nucleus formation cross section, σ_{CN}, is in each case equal to the total reaction cross section, σ_R. If this assumption is valid then, according to the independence hypothesis, the cross-section ratios, $\sigma(^4\text{He}, 3n)/\sigma_R(^4\text{He})$ and $\sigma(^3\text{He}, 3n)/\sigma_R(^3\text{He})$, should be equal to each other provided the comparison is made at the same excitation energy of the respective compound nuclei. For the purposes of this comparison it is reasonable to neglect the minor differences expected because of the different angular momentum distributions of the compound nuclei.

The results of this comparison are shown in Fig. 8. The values of σ_R were calculated with the ABACUS-2 code[22] using published values[28,29] of the optical-model parameters. It is seen that the values of σ/σ_R tend to be larger for the ^{4}He-induced reaction. The peak values of the ratios thus are 0.64 for ^{4}He and 0.43 for ^{3}He. This difference is most readily explained on the basis of a greater contribution of direct processes to the ^{3}He total reaction cross section, thereby making the quantity $\sigma_{CN}(^3\text{He})/\sigma_R(^3\text{He})$ smaller than $\sigma_{CN}(^4\text{He})/\sigma_R(^4\text{He})$. This behavior can be understood in view of the greater likelihood of stripping or pickup reactions for a ^{3}He projectile.

C. Comparison of Isomer Ratios with the Statistical Theory

The measured isomer ratios may be compared with the spin-dependent statistical theory. A method for the calculation of isomer ratios based on this theory was first developed by Vandenbosch and Huizenga.[30] The calculation was subsequently refined by Dudey and Sugihara[31] to include the effects of competitive charged-particle emission and limiting spin. The calculations usually have a number of adjustable parameters and the comparison with experiment serves to determine the best values of one or more of these quantities. Dudey and Sugihara[31] thus determined the values of the nuclear moment of inertia at excitation energies below 10 MeV. The validity of these estimates is questionable in view of some of the severe approximations made in the calculation. The analysis of the γ-ray cascade has posed particular problems because of the sensitivity of the results to the generally unknown details of the level scheme of the isomeric product. Our purpose in presenting the results of such a calculation is not to extract what are admittedly dubious values of nuclear parameters. Rather, the analysis offers a useful way of examining the dependence of the isomer ratios on such factors as the bombarding energy and the identity of the projectile.

The calculation closely resembles that described by Dudey and Sugihara.[31] The angular momentum distribution of the compound nucleus was evaluated with the ABACUS-2 code.[22] The changes in this distribution arising from neutron emission were determined with an adaptation of the EVAMCO code[32] and the effect of the γ-ray cascade was evaluated

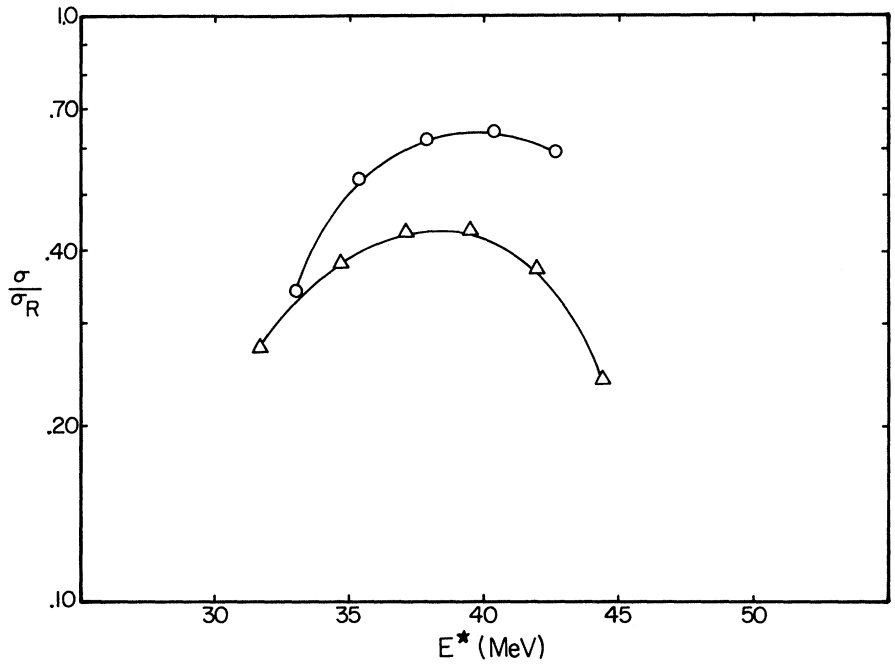

FIG. 8. Ratio of experimental cross section to the total reaction cross section as a function of compound-nucleus excitation energy. The (^{4}He, $3n$) reaction is represented by circles; the (^{3}He, $3n$) reaction by triangles.

with a program[33] based on the Vandenbosch-Huizenga formalism. The various parameters in the calculation were fixed in the manner described elsewhere[31,34] except for the nuclear moment of inertia at excitation energies below 10 MeV. This quantity was adjusted in order to fit the measured isomer ratio.

The results of the calculation are summarized in Fig. 9. An excellent fit to the experimental isomer ratios is obtained with the moments of inertia, $\mathcal{I}$, shown in the top half of the figure in terms of the rigid body values, $\mathcal{I}_r$. It is seen that the results for both reactions are consistent with the same value of $\mathcal{I}$ at all energies. Evidently, the various factors that lead to isomer ratios ranging from 0.7 to 8.7 are adequately accounted for in the calculation. It is particularly interesting to note that the same value of $\mathcal{I}$ can account for both the ^{3}He and ^{4}He results. We have shown in Sec. IV B that direct interactions make a much greater contribution to $\sigma_R(^3\mathrm{He})$ than to $\sigma_R(^4\mathrm{He})$. Since the angular momentum distribution of the compound nucleus is obtained from the optical model, it is based on the implicit assumption that the distributions of orbital angular momentum in the entrance channels for direct and compound-nuclear processes are similar. Since the isomer ratios for the two reactions can be fit with identical values of the various parameters, this assumption must be qualitatively correct.

D. Test of the Independence Hypothesis

The angular distribution results may be analyzed to yield the values of the average total kinetic energy of the emitted neutrons, T_n, and that of the emitted photons, T_γ. A comparison of these quantities for the ^{3}He- and ^{4}He-induced reactions then constitutes a test of the independence hypothesis.

The values of T_n may be obtained from $\langle V^2 \rangle$, the mean squared velocity imparted to the residual nucleus by isotropic neutron evaporation by means of the equation[5]

$$T_n = \tfrac{1}{8} \langle V^2 \rangle (A_T + A_B + A_R)^2 . \tag{5}$$

In turn, $\langle V^2 \rangle$ is related to the experimental $\langle \tan^2\theta_L \rangle$ values by the expression[6]

$$\langle \tan^2\theta_L \rangle = \sum_{n=1}^{\infty} \frac{2\langle V^{2n} \rangle}{(2n+1) v_{cn}^{2n}} . \tag{6}$$

The quantity v_{CN} is the velocity of the compound nucleus, obtained from the bombarding energy and conservation of momentum. The values of $\langle V^2 \rangle$ were determined by an iteration procedure. Three terms in the above expansion were required to obtain $\langle V^2 \rangle$ within 1% accuracy. The use of more than one term requires the assumption that $\langle V^{2n} \rangle = \langle V^2 \rangle^n$. The T_γ values were finally obtained as the difference between the total available energy and T_n:

$$T_\gamma = (E_{\mathrm{c.m.}} + Q) - T_n . \tag{7}$$

The results of this analysis are summarized in Table II. The uncertainties in the values of T_n and T_γ were estimated from the difference in the results obtained from bombardments at approximate-

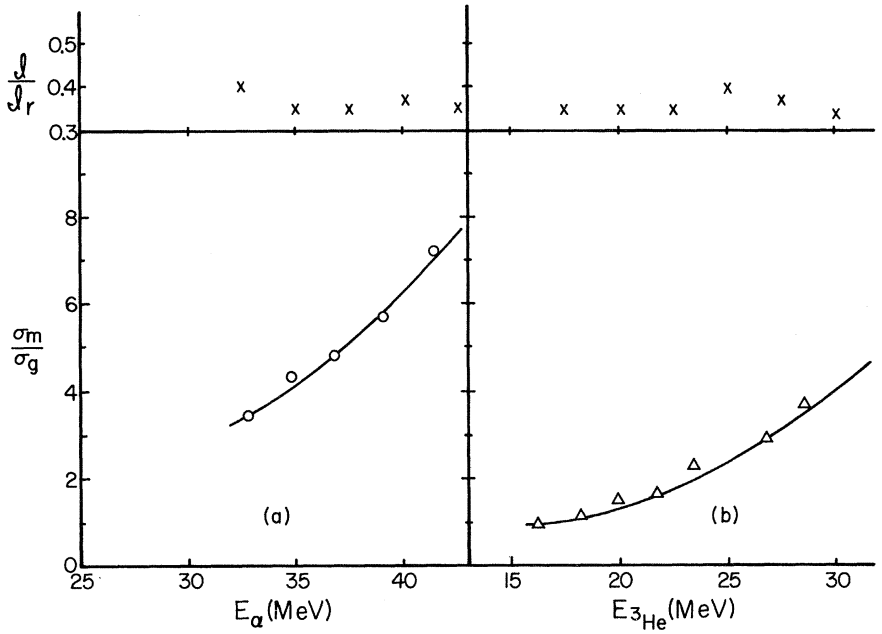

FIG. 9. Comparison of theoretical and experimental isomer ratios for the (a) ^{4}He- and (b) ^{3}He-induced reactions. Solid curve represents the calculated isomer ratio and the symbols are the experimental points. The upper portion of the figure gives the values of $\mathcal{I}/\mathcal{I}_r$ used to calculate the isomer ratios.

ly the same energy as well as from the total statistical uncertainty of the counting data. The mean uncertainty is 0.2 MeV for ^{137m}Ce and 0.6 MeV for ^{137g}Ce.

The validity of the independence hypothesis may be tested by comparing the values of T_n or T_γ derived for the two reactions at the same value of the available energy. Before presenting this comparison it is necessary to consider the differences in the angular momentum of the two systems. Since the reaction products are isomeric, we are particularly interested in the average angular momentum of those compound nuclei that deexcite to each isomeric state, denoted by $\langle J_c^m \rangle$ and $\langle J_c^g \rangle$. The isomer ratio program referred to in Sec. IV C was used to estimate these quantities.

Since the angular momentum distribution of the compound nucleus is modified by neutron and photon emission and since the isomer assignment is based on this modified distribution, it is difficult to make a direct determination of $\langle J_c^m \rangle$ and $\langle J_c^g \rangle$. In order to check the sensitivity of these quantities to the deexcitation process, approximate values of $\langle J_c^m \rangle$ and $\langle J_c^g \rangle$ were determined at each step of the deexcitation process. The results for the (^{4}He, $3n$) reaction at a compound-nucleus excitation energy of 42.8 MeV are summarized in Table III. The three entries refer, respectively, to the values obtained by apportioning between the two isomers the angular momentum distribution of the compound nucleus, that of the residual nucleus resulting from the emission of three neutrons, and that following the γ-ray cascade. It is seen that $\langle J_c^g \rangle$ is virtually independent of the method of calculation. On the other hand, the values obtained for $\langle J_c^m \rangle$ decrease as the deexcitation process proceeds. This result is a consequence of the shift of the angular momentum distribution of the com-

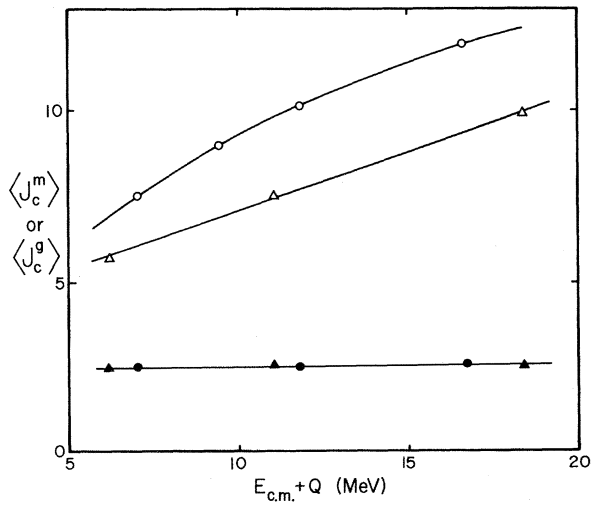

FIG. 10. Approximate values of the average angular momentum of compound nuclei leading to ^{137m}Ce and ^{137g} Ce. The circles refer to ^{4}He-induced reactions and triangles to ^{3}He-induced reactions. Open symbols show compound nuclei leading to ^{137m}Ce and shaded symbols those leading to ^{137g} Ce.

TABLE III. Average angular momentum of compound nuclei leading to ^{137m}Ce and ^{137g}Ce. The compound nucleus is formed in ^{4}He bombardment with an excitation energy of 42.8 MeV.

Method of calculation[a]	$\langle J_c^m \rangle$	$\langle J_c^g \rangle$
Method 1	13.5	2.4
Method 2	11.9	2.5
Method 3	10.0	2.5

[a]See text for explanation.

pound nucleus towards lower values by the emission of neutrons and photons. The values of $\langle J_c^g \rangle$ do not reflect this trend because the low spin of ^{137g}Ce restricts its formation to the lower end of the angular momentum distribution, whose shape is rather insensitive to the effect of neutron and photon emission. Of the three methods of calculating $\langle J_c^m \rangle$ it is clear that the first one overestimates its value while the third one underestimates it. Therefore method 2 was chosen as the best approximation to a calculation of $\langle J_c^m \rangle$ and $\langle J_c^g \rangle$.

The results of this computation are plotted in Fig. 10 for both ^{3}He and ^{4}He bombardments. It is seen that the same values of $\langle J_c^g \rangle$ are obtained for both reactions. Therefore, if a comparison of T_n and T_γ for ^{137g}Ce formation is made at the same excitation energy of the compound nuclei, the average angular momenta of the latter will also be equal. The T_n and T_γ values for the two reactions are plotted in Fig. 11. Within the limits of error, the results for ^{3}He and ^{4}He bombardments can be seen to fall on the same curve. This finding confirms the independence hypothesis for the reactions leading to ^{137g}Ce. In order to evaluate the sensitivity of this particular test of the hypothesis, the T_γ values for the two reactions were separately subjected to a linear least-squares fit and the standard deviations in T_γ were determined. This procedure will actually overestimate the standard deviations since there is no *a priori* reason to expect a linear variation of T_γ with energy. The standard deviation in the difference between the T_γ for the two reactions at intermediate available energies is 2.5 MeV. Our experiment is consequently sensitive to differences in energy partition of approximately this magnitude.

In the case of ^{137m}Ce formation Fig. 10 shows that $\langle J_c^m \rangle$ is larger for ^{4}He bombardments by 1 to 3 $\hbar$ units. One may therefore expect a difference in the T_n or T_γ values. The magnitude of this difference can be estimated on the assumption that the photon energy arises from the dissipation of the rotational energy of the compound nucleus. The rotational energy is obtained from the rigid-rotor model as

$$E_{\mathrm{rot}}{}^m = \frac{\langle J_c^m \rangle (\langle J_c^m \rangle + 1)\hbar^2}{2\vartheta_r}. \tag{8}$$

The expected difference in T_n or T_γ values is then obtained as the difference between the rotational energies obtained for ^{3}He and ^{4}He bombardment. This difference ranges from about 0.2 MeV for $(E_{\mathrm{c.m.}}+Q) = 6$ MeV to 0.6 MeV for $(E_{\mathrm{c.m.}}+Q) = 20$ MeV.

The values of T_n and T_γ for reactions leading to ^{137m}Ce are shown in Fig. 12. The width of the line drawn through the points corresponds to the difference in rotational energies and is thus a measure of the expected difference between the ^{3}He and ^{4}He points. Although the experimental points do scatter somewhat more than expected from the estimated uncertainties it does appear that the T_γ values from the ^{4}He experiments are slightly larger than those from the ^{3}He ones, in agreement with the theoretical estimate. Our conclusion is that the reactions leading to ^{137m}Ce also confirm the independence hypothesis with comparable sensitivity as those leading to ^{137g}Ce.

A more sensitive test of the relation between angular momentum and energy dissipated in photon emission than is afforded by the data in Fig. 12 can be obtained from a comparison of the T_n or T_γ values associated with the formation of ^{137m}Ce and ^{137g}Ce in the same reaction. As indicated in Fig. 10, the differences between $\langle J_c^m \rangle$ and $\langle J_c^g \rangle$ for a given projectile range from 3 to 10 $\hbar$ units so that the expected effect is much larger. As before, the expected difference in photon energies is obtained by application of Eq. (8) to the data shown in Fig. 10. The experimental values of ΔT_γ are obtained by direct subtraction of the T_γ values for ^{137g}Ce from those for ^{137m}Ce at the same bombarding energy. The results are shown in Fig. 13. Because

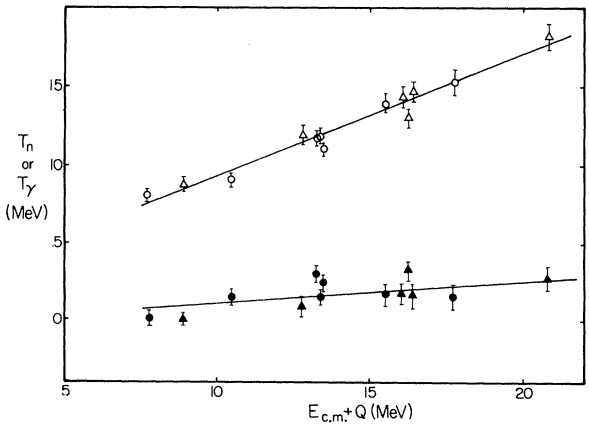

FIG. 11. Comparison of T_n and T_γ for ^{137g}Ce from (^{4}He, $3n$) and (^{3}He, $3n$) reactions. Triangles represent ^{3}He; circles, the ^{4}He reactions. Open symbols refer to T_n and shaded symbols to T_γ.

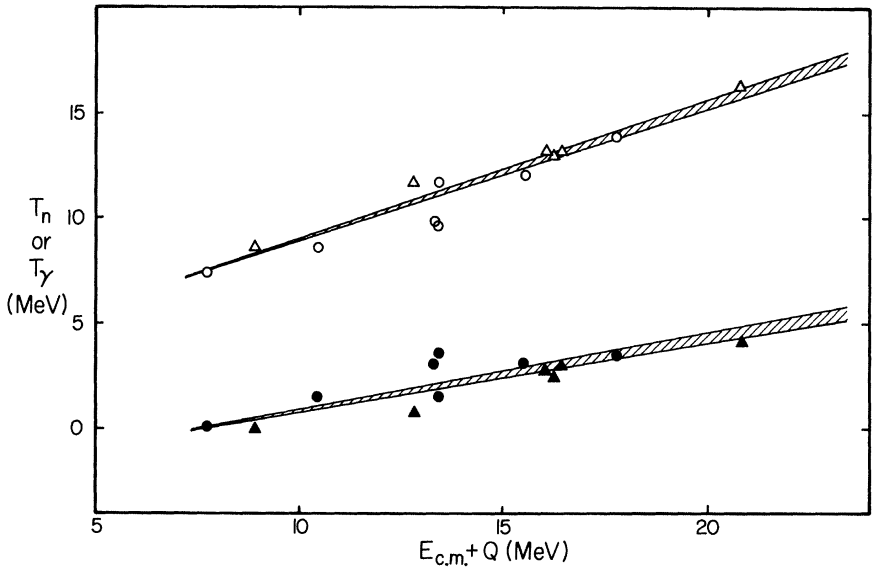

FIG. 12. Comparison of T_n and T_γ for ^{137m}Ce from the (^{4}He, $3n$) reactions. Symbols have same meaning as in Fig. 11. The widths of the lines drawn through the points correspond to the expected difference between ^{4}He and ^{3}He reactions.

of the very small difference in Q values for the formation of ^{137m}Ce and ^{137g}Ce, the experimental points are plotted at the average values of $E_{c.m.}+Q$. Within the rather large uncertainties introduced by the subtraction of T_γ values, the experimental points are in satisfactory agreement with the theoretical curve.

V. CONCLUSIONS

The ^{136}Ba(^{4}He, $3n$) and ^{137}Ba(^{3}He, $3n$) reactions have been shown to be predominantly compound nuclear over the energy interval studied, as evidenced by average range measurements. The excitation functions differed in magnitude from previous measurements,[7,8] but peaked at approximate-

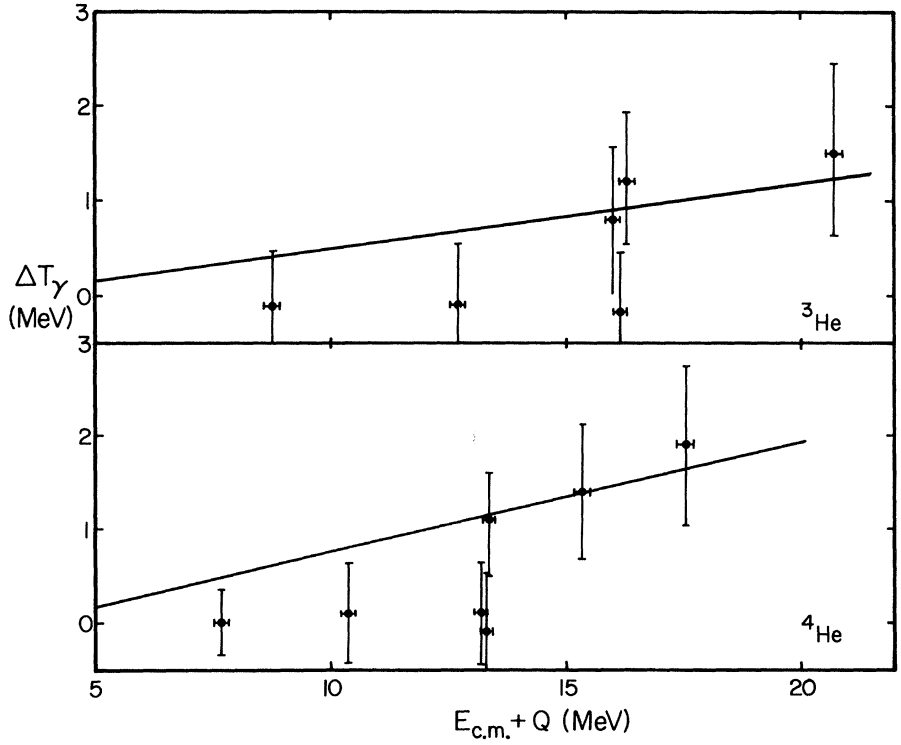

FIG. 13. Difference between T_γ for reactions leading to ^{137m}Ce and ^{137g} Ce. Symbols represent the experimental points and the solid line is from the theoretical calculation.

ly the same energy as reported by KS.[7] The isomer ratios for both reactions agreed quite well with the results of KS[7] and with a calculation based on the statistical theory. Comparison of the (^{4}He, $3n$) and (^{3}He, $3n$) cross sections reveals that the probability of direct interactions in ^{3}He-induced reactions is larger than in those induced by ^{4}He.

The angular distributions of the recoil products were used to derive the values of T_n and T_γ. Comparison of these quantities for ^{137g}Ce formation permits the simultaneous equalization of the excitation energy and angular momentum of the compound nuclei formed in ^{3}He and ^{4}He bombardment, and thereby makes a correct test of the independence hypothesis possible. The partition of the available energy between neutrons and photons is found to be independent of projectile to within 2.5 MeV. The quantitative relationship between photon energy and angular momentum of the compound nucleus is demonstrated by a comparison of the results for ^{137m}Ce and ^{137g}Ce for both ^{3}He- and ^{4}He-induced reactions.

The cooperation of M. Oselka and the operating crew of the Argonne National Laboratory 60-in. cyclotron is gratefully acknowledged. We wish to thank Dr. L. Glendenin for the use of his calibrated x-ray detector. The help of D. G. Swanson in some phases of this work is acknowledged. We wish to thank Dr. R. Reedy and Professor J. M. Miller for a copy of the EVAMCO code. The LSS ranges were kindly supplied by Dr. H. E. Schiøtt.

---

*Work supported by the U. S. Atomic Energy Commission.

†Submitted in partial fulfillment of the requirements for the Ph.D. degree in the Department of Chemistry, Purdue University.

[1]S. N. Ghosal, Phys. Rev. 80, 939 (1950).

[2]N. T. Porile, S. Tanaka, H. Amano, M. Furukawa, S. Iwata, and M. Yagi, Nucl. Phys. 43, 500 (1963).

[3]J. R. Grover and R. J. Nagle, Phys. Rev. 134, B1248 (1964).

[4]J. M. D'Auria, M. J. Fluss, G. Herzog, L. Kowalski, J. M. Miller, and R. C. Reedy, Phys. Rev. 174, 1409 (1968).

[5]G. N. Simonoff and J. M. Alexander, Phys. Rev. 133, B105 (1964).

[6]M. Kaplan and V. Subrahmanyam, Phys. Rev. 153, 1186 (1967).

[7]R. L. Kiefer and K. Street, Jr., Phys. Rev. 173, 1202 (1968); R. L. Kiefer, Lawrence Radiation Laboratory Report No. UCRL 11049, 1963 (unpublished).

[8]T. Matsuo, J. M. Matuszek, Jr., N. D. Dudey, and T. T. Sugihara, Phys. Rev. 139, B886 (1965).

[9]G. B. Saha and N. T. Porile, Phys. Rev. 149, 880 (1966).

[10]G. B. Saha and N. T. Porile, Phys. Rev. 151, 907 (1966).

[11]C. F. Williamson, J. Boujot, and J. Picard, Commissariat à l' Energie Atomique Report No. CEA-R3042, 1966 (unpublished).

[12]S. Bjørnholm, Nucl. Instr. Methods 5, 196 (1959).

[13]L. E. Glendenin, K. F. Flynn, R. F. Buchanan, and E. P. Steinberg, Anal. Chem. 27, 59 (1955).

[14]C. M. Lederer, J. M. Hollander, and I. Perlman, *Table of Isotopes* (John Wiley & Sons, Inc., New York, 1967), 6th ed.

[15]A. H. Wapstra, G. J. Nijgh, and R. Van Lieshout, *Nuclear Spectroscopy Tables* (North-Holland Publishing Company, Amsterdam, The Netherlands, 1959), Chap. 7.

[16]D. G. Swanson and N. T. Porile, Nucl. Phys. A144, 344 (1970).

[17]N. T. Porile and G. B. Saha, Phys. Rev. 158, 1027 (1967).

[18]I. Fujiwara and N. T. Porile, Phys. Rev. 173, 1055 (1968).

[19]W. Parker and A. Falk, Nucl. Instr. Methods 49, 220 (1967).

[20]D. G. Swanson and N. T. Porile, Nucl. Phys. A144, 355 (1970).

[21]K. Hohmith, G. Mueller, and J. Schintlemeister, Nucl. Phys. 48, 209 (1963).

[22]E. Auerbach, Brookhaven National Laboratory Report No. BNL 6562, 1962 (unpublished).

[23]D. M. Montgomery and N. T. Porile, Nucl. Phys. 130, 65 (1969).

[24]P. Wong, P. J. Daly, and N. T. Porile, to be published.

[25]J. H. E. Mattauch, W. Thiele, and A. H. Wapstra, Nucl. Phys. 131, A119 (1968).

[26]J. Lindhard, M. Scharff, and H. E. Schiøtt, Kgl. Danske Videnskab. Selskab, Mat.-Fys. Medd. 33, No. 14 (1963).

[27]L. Winsberg and J. M. Alexander, Phys. Rev. 121, 518 (1961).

[28]J. R. Huizenga and G. T. Igo, Nucl. Phys. 29, 462 (1962).

[29]P. E. Hodgson, in *Direct Interactions and Nuclear Reaction Mechanisms*, edited by E. Clementel and C. Villi (Gordon and Breach, New York, 1962), p. 103.

[30]R. Vandenbosch and J. R. Huizenga, Phys. Rev. 120, 1313 (1960).

[31]N. D. Dudey and T. T. Sugihara, Phys. Rev. 139, B896 (1965).

[32]R. Reedy, private communication.

[33]W. L. Hafner, J. R. Huizenga, and R. Vandenbosch, Argonne National Laboratory Report No. ANL-6662, 1962 (unpublished).

[34]D. M. Montgomery, Ph.D. thesis, Purdue University, 1969 (unpublished).